Colloidal System To Explore Structural and Dynamical Transitions in Rod Networks, Gels, and Glasses

Georgina M. H. Wilkins,*,† Patrick T. Spicer,‡ and Michael J. Solomon†

†*Department of Chemical Engineering, University of Michigan, 2300 Hayward Street, Ann Arbor, Michigan 48109, and* ‡*Corporate Engineering, The Procter and Gamble Company, 8256 Union Centre Boulevard, West Chester, Ohio 45069*

We introduce a model system consisting of self-assembled polyamide anisotropic colloids suspended in an aqueous surfactant solution for studies of the dynamics of rod networks, gels, and glasses. The colloidal particles are formed by recrystallization of a polyamide from an aqueous surfactant phase at temperatures from 59 to 100 °C. The aspect ratio increases monotonically with temperature from $T = 59$ °C to $T = 100$ °C and rods with an aspect ratio $r = 8 \pm 1$ to $r = 306 \pm 14$ form. We show by confocal laser scanning microscopy and dynamic light scattering a structural transition from dilute rod behavior with diffusive dynamics to a homogeneous network structure with increasingly slow dynamics as the volume fraction is increased. Furthermore, increasing the aspect ratio of rods induces a similar structural transition from dilute rod behavior to a network structure, although at a lower volume fraction. Finally, we vary the pair potential between the rods by a polymer-induced depletion interaction and thereby observe an unexpected network-to-bundle transition. The bundles are several rod diameters wide and 1−2 rod lengths long. The rods appear to be ordered nematically within each bundle. The bundling transition leads to an order of magnitude decrease in the storage modulus of the suspensions. The results can be applied to develop strategies for complex fluid stabilization as well as for fundamental studies of rod gelation and vitrification.

Introduction

The fundamental physics of microstructural transitions in rod suspensions is of interest because of the implications of such transitions for rheological modification. The effect of anisotropy and the effect of microstructure induced by anisotropy on dynamical transitions such as gelation and the glass transition are also of broad interest in soft matter physics. However, there are few experimental data available to test recent simulations and theoretical studies of the interaction of colloidal anisotropy, microstructure, and slow dynamics.[1−5] One obstacle is that no simple experimental systems exist with independently tunable aspect ratios and interaction potentials that can be made in quantities sufficient for rheological study. In this study, we present a model system produced by surfactant-templated recrystallization of polyamide to address this gap. We use dynamic light scattering (DLS), confocal laser scanning microscopy (CLSM), and rheology to study the rod microstructure and dynamics in an aqueous surfactant solution. This system creates a pathway to develop complex fluid formulations with tunable physical properties useful in, for example, consumer products. To explore this pathway, we probe how particle shape, interaction strength, and volume fraction (ϕ) control the microstructure and dynamics of these rod suspensions.

Rods add structure to consumer products and other materials either by aggregating or entangling to form homogeneous and heterogeneous networks.[6,7] Rodlike nanocolloids are often preferable to spheres because they modify rheology more efficiently; their anisotropic excluded volume results in lower percolation thresholds, requiring lower particle loading for equivalent material properties.[8] The gelation transition for rods is highly aspect ratio-dependent and occurs at volume fractions that are far lower than for spheres.[9] Although some empirical results are available,[9−12] a full picture of how physical properties such as the aspect ratio and interaction potential interact to yield networks and gel microstructures is not yet available.

Thus, there is a need for a model nanocolloidal system in which the effect of such parameters on structure and dynamics can be explored. Such a system must comprise monodisperse, Brownian particles that are simple to synthesize in quantities that allow mechanical rheometry studies. Control of the rod aspect ratio (where the aspect ratio, r, is the length of the rod divided by the diameter of the rod) is also necessary, as is the ability to vary colloidal pair potential interactions using, for example, depletion forces. Finally, the system should also be density- and index-matched to the solvent to allow structural and dynamical studies with methods such as small angle light scattering (SALS), DLS, and CLSM.

Previously developed model rod systems that satisfy some of these constraints include boehmite spindles,[11,13,14] hematite spindles,[12,15] poly(methyl methacrylate) (PMMA) elongated

*To whom correspondence should be addressed. E-mail: gmhw@umich.edu.

(1) Doi, M.; Edwards, S. *Dynamics of Polymeric Liquids*, 1st ed.; Oxford Science Piblications: Oxford, 1986.
(2) Morse, D. *Phys. Rev. E* **1998**, *58*, 1237.
(3) Glaser, J.; Hallatschek, O.; Kroy, K. *Eur. Phys. J. E* **2008**, *26*, 123–136.
(4) Yatsenko, G.; Schweizer, K. S. *Langmuir* **2008**, *24*, 7474–7484.
(5) Pfleiderer, P.; Milinkovic, K.; Schilling, T. *Europhys. Lett.* **2008**, *84*, 16003.
(6) Wierenga, A.; Philipse, A. *Langmuir* **1998**, *14*, 49–54.
(7) Shankar, V.; Pasquali, M.; Morse, D. *J. Rheol.* **2002**, *46*, 1111–1154.

(8) Vigolo, B. *Science* **2005**, *309*, 920–923.
(9) Mohraz, A.; Solomon, M. *J. Colloid Interface Sci.* **2006**, *300*, 155–162.
(10) Varga, S.; Fraden, S. *J. Chem. Phys.* **2007**, *127*, 154902.
(11) Wierenga, A.; Philipse, A.; Lekkerkerker, H.; Boger, D. *Langmuir* **1998**, *14*, 55–65.
(12) Solomon, M.; Boger, D. *J. Rheol.* **1998**, *42*, 929–949.
(13) Buitenhuis, J.; Dhont, J.; Lekkerkerker, H. *Macromolecules* **1994**, *27*, 7267–7277.
(14) Mohraz, A.; Moler, D.; Ziff, R.; Solomon, M. *Phys. Rev. Lett.* **2004**, *92*, 155503.
(15) Matijevic, E. *Annu. Rev. Mater. Sci.* **1985**, *15*, 483–516.

ellipsoids,[16–18] poly(benzyl-L-glutamate) (PBLG),[19–21] calcium carbonate rods,[22] carbon nanotubes (CNTs),[23–28] *f*-actin,[29] and *fd* virus.[30,31] For example, the boehmite system has been used to show that rod fractal microstructures differ from spheres and that gelation volume fractions are dependent on the aspect ratio.[9,13,14] Hematite spindles have been used to probe the effect of aspect ratio on the viscosity of concentrated rod suspensions.[12] Theoretical classification of rigid rods have been approximated by stiff polymers like PBLG.[19,21] Suspensions of rodlike calcium carbonate have been used to investigate the role of aspect ratio and ϕ on the onset of shear thickening behavior via hydrocluster formation.[22] CNTs have also been used to investigate rod rheological signatures, extending the aspect ratio range of boehmite, hematite, and calcium carbonate over 30–1000.[24] Hematite, boehmite, calcium carbonate, and CNTs are all polydisperse to varying degrees: boehmite (25–40%),[13,14] hematite (<20%),[12] and calcium carbonate (20% for $r \sim 2$ and $\sim 40\%$ for $r \sim 6$).[22] CNTs also exhibit significant polydispersity,[24] complicating the characterization of physical properties as well as comparison to theory and simulation. Finally, boehmite and CNTs are difficult to density match in common solvents. Poor density matching results in rod sedimentation and can complicate their use as model systems for the study of rod suspensions.

In addition to the synthetic rods discussed above, rod-shaped viruses[30,31] and *f*-actin[29] rods can be applied to the general study of rod suspension microstructure and dynamics. Recently, Zhang and co-workers used a sticky rodlike system comprised of poly(N-isopropylacrylamide) (PNIPAM)-coated *fd* virus to study the effect of particle shape and interaction strength on gelation in isotropic and nematic gels.[32]

Model rod systems, particularly ones in which *r* can be varied, can contribute to the testing of rod network, gel, and glass theories. Onsager's seminal paper on structural phase transitions in solutions of anisometric particles can be used to predict order–disorder transitions in colloidal rod suspensions.[33–35] Theories describing the rheology of semiflexible and rigid rod networks include the tube model of de Gennes and Doi and Edwards.[1] Here, the surrounding network confines a rigid rod in a tube. Rotational dynamics of the rod in the tube lead to linear viscoelasticity in which the longest relaxation times scale as $\tau \propto r^4 \phi^2$.[1] Morse and MacKintosh predicted linear viscoelasticity for entangled solutions of semiflexible polymers by modeling them as wormlike chains and using the tube model to account for entanglements in the system. At high frequencies, the dynamic modulus scales as $\omega^{3/4}$.[2,36] The model may also be used to understand the viscoelasticity of isotropic solutions of wormlike chains.[2] Recent work of Glaser et al. predicts the dynamic structure factor for glassy solutions of stiff polymers using the wormlike chain model.[3,37] Finally, Yatsenko and Schweizer have developed a theory to predict that the glass transition is a decreasing function of the aspect ratio (for $r > 2$) for isotropic suspensions of rigid rods.[4]

Here, we present the preparation of a model system comprised of polyamide nanocolloidal rods with tunable aspect ratios and pair potentials. The rods are large enough to be observed with optical microscopy but are Brownian, enabling us to use photon correlation spectroscopy to explore the structure and dynamics of semidilute and concentrated suspensions. We show that increasing the pair potential between the rods creates dramatic structural changes including that of rod bundling. Such structural changes are strongly correlated to the dynamics and bulk rheology of the suspensions.

Materials and Methods

Preparation of Model Nanorods. Rod suspensions were prepared using a polyamide powder (Disparlon 6650, King Industries, Norwalk, CT) dispersed in aqueous surfactant solution. Rods were produced in two surfactant solutions: The first contained linear alkyl benzene sulfonate (16.0% wt), water, and trace amounts of buffering ingredients (Procter and Gamble Co., West Chester, OH), and the second contained 16.0% wt sodium dodecylbenzenesulfonate (technical grade, Aldrich Chemical Co., Inc., Milwaukee, WI) and approximately 84.0% wt DI water. The solutions each had a pH of $\approx$7.5. Although these two surfactant solutions produced comparable rods, in general, other surfactant phases did not produce rodlike particles. All data presented here are for suspensions prepared with the first surfactant solution.

The synthesis procedure was as follows: Rod suspensions were prepared in 5 mL batches and were mixed in 22 mL vials. A 4.95 $\pm$ 0.01 g amount of surfactant solution was added to the vial followed by 0.05 $\pm$ 0.01 g of polyamide powder. The final weight ratio was water:surfactant:polyamide, 83:16:1. A 1 cm magnetic stir bar was carefully placed into the vial. The vial was sealed using a Teflon-coated screw top and suspended in a large silicon oil vat. The vat was placed on a stirrer/hot plate (Corning Inc., Corning, NJ) providing temperature control inside the vial of $\pm$0.2 °C. The samples were stirred for 15 min at particular temperatures between $59 < T < 100$ °C. Because the rods have a density comparable to the surfactant solution ($\rho_{rod} = \rho_{solvent} = 0.99 \pm 0.01$ g/cm^3), no significant rod sedimentation occurred over time. Unless otherwise stated, ϕ of rods in the synthesis solutions was 0.01; however, it is noted that we were able to synthesize monodisperse rod suspensions at volume fractions up to 0.03. For $\phi > 0.03$, the solution viscosity increased to the point that the magnetic stir bar could not adequately mix the entire sample. To assess the significance of charge on the rods, we measured the mobility of the rods at dilute concentrations using a Zetasizer Nano Series (Malvern, United Kingdom) in a high salt limit (0.1 M potassium chloride) where the Smoluchowski equation can be applied. The Smoluchowski equation is valid for a particle of arbitrary shape. In this case, we measured a ζ potential of -36 mV, indicating that surface charge likely contributes to their colloidal stability. Rod suspensions of volume fractions from $0.0005 < \phi < 0.01$ were prepared from stock suspensions described above. For the range of aspect ratios ($8 < r < 79$)

(16) Mohraz, A.; Solomon, M. *Langmuir* **2005**, *21*, 5298–5306.
(17) Ho, C.; Keller, A.; Odell, J.; Ottewill, R. *Colloid Polym. Sci.* **1993**, *271*, 469–479.
(18) Keville, K.; Franses, E.; Caruthers, J. *J. Colloid Interface Sci.* **1991**, *144*, 103–126.
(19) Mead, D.; Larson, R. *Macromolecules* **1990**, *23*, 2524–2533.
(20) DeLong, L.; Russo, P. *Macromolecules* **1991**, *24*, 6139–6155.
(21) Wagner, N.; Walker, L.; Hammouda, B. *Macromolecules* **1995**, *28*, 5075–5081.
(22) Egres, R.; Wagner, N. *J. Rheol.* **2005**, *49*, 719–746.
(23) Hough, L.; Islam, M.; Hammouda, B.; Yodh, A.; Heiney, P. *Nano Lett.* **2006**, *6*, 313–317.
(24) Fan, Z.; Advani, S. *J. Rheol.* **2007**, *51*, 585–604.
(25) Schilling, T.; Jungblut, S.; Miller, M. A. *Phys. Rev. Lett.* **2007**, *98*, 108303.
(26) Zakri, C.; Poulin, P. *J. Mater. Chem.* **2006**, *16*, 4095.
(27) Hobbie, E. K.; Fry, D. J. *Phys. Rev. Lett.* **2006**, *97*, 036101.
(28) Duggal, R.; Pasquali, M. *Phys. Rev. Lett.* **2006**, *96*, 246104.
(29) Lieleg, O.; Claessens, M. M. A. E.; Heussinger, C.; Frey, E.; Bausch, A. R. *Phys. Rev. Lett.* **2007**, *99*, 8102.
(30) Dhont, J. K. G.; Lettinga, M. P.; Dogic, Z.; Lenstra, T. A. J.; Wang, H.; Rathgeber, S.; Carletto, P.; Willner, L.; Frielinghaus, H.; Lindner, P. *Faraday Discuss.* **2002**, *123*, 157–172.
(31) Purdy, K. R.; Varga, S.; Galindo, A.; Jackson, G.; Fraden, S. *Phys. Rev. Lett.* **2005**, *94*, 057801.
(32) Zhang, Z.; Krishna, N.; Lettinga, M. P.; Vermant, J.; Grelet, E. *Langmuir* **2009**, *24*, 9636–9641.
(33) Onsager, L. *Ann. N. Y. Acad. Sci.* **1949**, *15*, 627–659.
(34) Bruggen, M. P. B. V.; Dhont, J. K. G.; Lekkerkerker, H. N. W. *Macromolecules* **1999**, *32*, 2256–2264.
(35) Maeda, H.; Maeda, Y. *Nano Lett.* **2007**, *7*, 3329–3335.

(36) Gittes, F.; MacKintosh, F. *Phys. Rev. E* **1998**, *58*, 1241–1244.
(37) Semmrich, C.; Storz, T.; Glaser, J.; Merkel, R.; Bausch, A.; Kroy, K. *Proc. Natl. Acad. Sci.* **2007**, *104*, 20199–20203.

studied, these volume fractions corresponded to the dilute regime as described by Doi and Edwards for rigid rods.[1,38]

The volume fraction at which a nematic phase is stable can be calculated using the random contact model.[39] For spherocylinders, $\phi \frac{L}{D}\left[4\frac{D}{L} + \frac{3(L/D)}{3(L/D)+2}\right] = \langle c \rangle$ where L is the length of the rod, D is the diameter of the rod, and $\langle c \rangle$ is the average number of contacts per particle, which is 4.19 for a stable nematic phase. To test if these theoretical ideas about the dilute/semidilute transition and the order/disorder transition were appropriate to apply to the system, we experimentally measured the location of the isotropic/nematic transition for the particular case of the $r = 15$. We found that a stable nematic phase was obtained for rods with an aspect ratio of $r = 15$ using the centrifugation force as an effective gravitational field to order rod assemblies.[40] A custom-made vial (as in ref 40) was filled with a rod suspension ($r = 15$) and placed in a desktop device (Allegra 21R, Beckman Coulter, Inc., United States) at 10000 rpm for 24 h. The volume fraction of the rod sediment was measured and found to be $\phi = 0.26$. This measurement is in good agreement with the random contact model, which predicts a stable nematic phase for rods of $r = 15$ at volume fractions $\phi_N = 0.23$ or greater.

Edwards and Evans predicted that the volume fraction of the glass transition in rigid rod suspensions scales equivalently to the volume fraction of the I−N transition.[41] Because the suspensions studied here are more than an order of magnitude lower in volume fraction than the I−N transition, the suspensions that exhibit arrested dynamics in this study are likely attractive gels, rather than glasses. However, by concentrating the rods using centrifugation or dialysis, the polyamide rod system could equally well be applied to study rod glasses using a similar methodology that we have applied here for gels.

Attractions were induced in the rod suspensions by the addition of nonadsording polymer, poly(ethylene oxide) (PEO) which acts as a depletant.[42] The polymer solutions were comprised of varying amounts of PEO (Aldrich Chemical Co., Inc.) of molecular weight $M_w = 100000$ g/mol, a radius of gyration $R_g = 17.6$ nm, and a critical overlap concentration $c^* = 7000$ ppm,[43] and added to DI water. Here, $c^* = 3M_w/4\pi N_A R_g^3$, where N_A is the Avogadro constant.[43] The polymer solutions were gently rolled for 24 h before being added to the stock rod suspensions. The stock rod suspensions were prepared as described above and then diluted to a volume fraction of 0.001 using the polymer solutions. The suspensions were subsequently rolled (rotating at < 3 rpm to facilitate mixing but avoid shearing) for 24 h. Here, R_g/b is fixed at 0.22, where b is the minor axis of the rod. The strength of the depletion interaction is a function of the size of the depletant and its concentration.[42] The latter is typically quantified by the ratio c/c^* where c^* is the overlap concentration ($c^* = 7000$ ppm for this polymer). For this study, the polymer concentration was varied from $0.014 < c/c^* < 1.19$.

Microscopy. Reflection CLSM (Leica TCS SP2, Leica, Bannockburn, IL) was conducted on an inverted microscope (Leica DMIRE2) with a 100× oil immersion objective with a numerical aperture of 1.4. Images were collected using reflection mode with laser excitation at $\lambda = 488$ nm. Rod suspensions were placed in 1 mL vials with the lower portion of the vial replaced with a coverslip to maximize the portion of the working distance available for imaging. Images were captured at least 5 μm from the coverslip. The optical resolution in the plane of the objective was ±240 nm and ±550 nm in the direction perpendicular to the objective. The objective plane was parallel to the coverslip. The

pixel size was typically 122×122 nm^2, giving an image size 62.46×62.46 μm^2. CLSM was used to identify the length of the individual rods in suspension and to assess the macroscopic and microscopic structure of the suspensions. Occasionally, an area of increased brightness was observed in the center of the field of view. This is typical of the reflection method.[44]

Atomic force microscopy (AFM) was used to measure the dimensions of the rods. A Nanoscope IIIa phase microscope (Veeco Instruments Inc., Plainview, NY) coupled with a J scanner at a scan speed of 1 Hz was used. A silicon cantilever (NSC15/no Al, MikroMasch, San Jose, CA) with drive frequency $f = 275.94$ Hz probed the sample. The samples were prepared by placing a dilute droplet of the rod suspensions on a clean silicon substrate[45] and leaving the sample to dry in ambient conditions. The scanner typically probed a 10×10 μm^2 area of the sample. Because of the relatively small scan size of AFM, only the average diameters of the rods were extracted from the measured height profile.

DLS. DLS was performed on a compact goniometer system with a multitau correlator with a minimum delay time of 12.5 ns (ALV-5000E, ALV, Langen, Germany). The samples were placed in a clean cylindrical vial in a temperature-controlled vat of refractive index matching toluene. Incident light of wavelength $\lambda = 488$ nm (Innova 70C, Coherent Inc., Santa Clara, CA) was scattered by the sample, and the scattered light was collected by a detector at wave vector $q = 13.1$ μm^{-1}, where $\theta = 45°$. Using the correlator, the time-averaged normalized autocorrelation function, $g_2(q,t) = \langle I(q,0)I(q,t)\rangle/\langle I(q)\rangle_e^2$, was measured. DLS is a useful tool to characterize the dynamic structure factor, $f(q,t)$, from $g_2(q,t)$. $f(q,t)$ quantifies the spatial decorrelation of particle positions over time. At dilute conditions, for example, it is a function of particle diffusivity. It is a key quantity for studying phenomena such as the glass[46] and gelation transitions.[47]

For ergodic samples, $f(q,t)$ can be measured directly from the autocorrelation function by applying the Siegert relationship, $g_2(q,t) = 1 + \beta[f(q,t)]^2$, where β is the coherence factor, which has a magnitude from 0 to 1. β is related to the ratio of the speckle size and the detector size. For nonergodic samples, the Siegert relationship cannot be used; however, Pusey and van Megan[48] developed a method for extracting the dynamic structure factor from a single measurement of $g_2(q,t)$ and identifying the ratio of time and ensemble averages of the scattered intensities $I(q)^t/I(q)^e$. Here, $I(q)^t$ is the time-averaged scattered intensity, and $I(q)^e$ is the ensemble-averaged intensity. These quantities come from a measurement of the average scattered intensity during the experiment $[I(q)^t]$ and a measurement of the scattered intensity in a separate short experiment in which the vial is rotated to explore the entire ensemble of speckles in the material $[I(q)^e]$.

Rheology. Linear viscoelasticity of rod suspensions was measured on a ARG2 stress-controlled rheometer (TA Instruments, New Castle, DE). A cone and plate geometry ($\alpha = 2°$, $d = 20$ mm, and truncated at 48 μm) was coupled with a Peltier plate. A solvent trap, internally padded with adsorbent material soaked in water, ensured minimal solvent evaporation for the duration of the experiment. Experiments were performed at $T = 25$ °C. Instrument inertial constraints and transducer sensitivity produced an accessible frequency range of about 2 decades in ω (rad/s).[49]

Results

Polyamide Rod Characterization. The length and diameter of the rods were measured using reflection CLSM and AFM, respectively. Figure 1 shows reflection CLSM and AFM micrographs for rod suspensions prepared at 86.9 °C (at left) and

(38) Larson, R. *The Structure and Rheology of Complex Fluids*, 1st ed.; Oxford University Press: New York, 1999.
(39) Philipse, A. *Langmuir* **1996**, *12*, 1127–1133.
(40) Mukhija, D. Ph.D. Thesis, University of Michigan, 2009.
(41) Edwards, S.; Evans, K. *J. Chem. Soc. Faraday Trans. 2* **1982**, *78*, 113–121.
(42) Asakra, S.; Imai, N.; Oosawa, F. *J. Polym. Sci.* **1954**, *13*, 499–510.
(43) Brown, W. *Dynamic Light Scattering: The Method and Some Applications*, 1st ed.; Oxford University Press: Oxford, 1993.
(44) Paddock, S. *Biotechniques* **2002**, *32*, 274–278.
(45) Critchley, K.; Zhang, L.; Fukushima, H.; Ishida, M.; Shimoda, T.; Bushby, R. J.; Evans, S. D. *J. Phys. Chem. B* **2006**, *110*, 17167–17174.
(46) van Megen, W.; Underwood, S. *Phys. Rev. E* **1994**, *49*, 4206.
(47) Zaccarelli, E. *J. Phys.: Condens. Matter* **2007**, *19*, 323101.
(48) Pusey, P.; van Megen, W. *Phys. A* **1989**, *157*, 705–741.
(49) Bird, R.; Armstrong, R.; Hassager, O. *The Theory of Polymer Dynamics*, 1st ed.; John Wiley and Sons: New York, 1987.
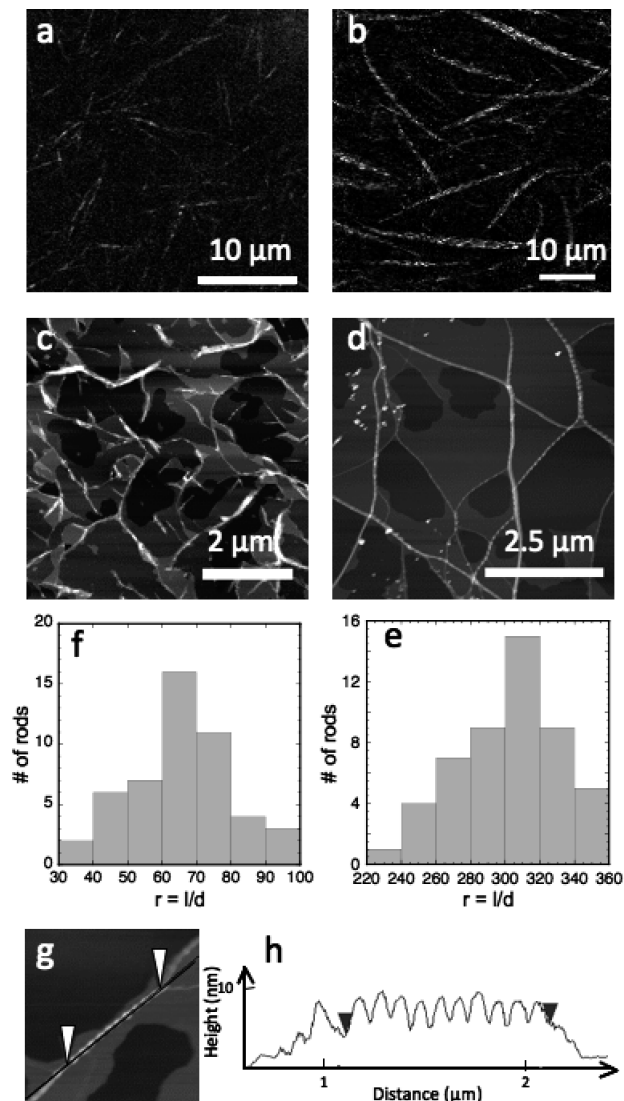
Figure 1. Micrographs of rods prepared at 86.9 (LHS) and 100.0 °C (RHS). (a) and (b) reflection CLSM of rod suspensions. (c and d) AFM micrographs of dried thin films of the rod suspensions. (e and f) The distribution of rod aspect ratio as measured from CLSM (rod length) and AFM (rod diameter) for $T = 86.9$ °C and $T = 100.0$ °C, respectively. (g) Micrograph showing that the rod has surface texture; the rod has the appearance of a helical ribbon. The pitch length is approximately 100 nm. Panel h corresponds to the height profile along the surface of the rod vs the position along the rod in panel g.

100.0 °C (at right). Figure 1a,b shows confocal micrographs, which are used to identify the rod lengths. Rod lengths range from 1 to 25 μm, depending on the preparation temperature of the suspension. Notice that short rods ($r < 100$) are straight, whereas long rods ($r > 100$) display some curvature. Because reflection CLSM lacks the necessary resolution, AFM was used to measure the average rod diameters. We found that there was minimal swelling of the rods in solution by measuring the rod length in both wet and dry suspensions using differential interference contrast microscopy (CytoViva, Auburn, AL). Figure 1c,d shows topographical micrographs of samples dried onto silicon substrates from AFM. The AFM height profile is used to determine the average diameter of the rods. Figure 1e,f displays the distribution of aspect ratios obtained by combining rod lengths from CLSM and rod diameters from AFM. The average aspect ratio for rods prepared at 86.9 °C is 62 ± 4 and for rods prepared

Table 1. Rod Dimensions for Rods Presented in Figure 2

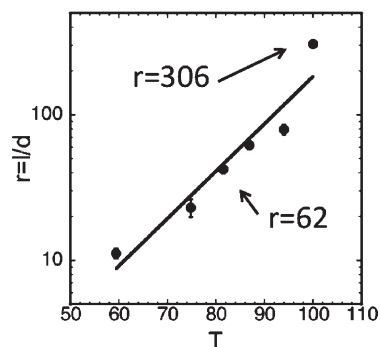| T (°C)	$r = l/d$	l (μm)	d (nm)
59.4	11 ± 1	0.9 ± 0.1	80 ± 3
74.8	23 ± 3	2.0 ± 0.2	95 ± 4
81.5	42 ± 3	4.1 ± 0.2	96 ± 4
84.0	54 ± 3	4.9 ± 0.1	90 ± 5
86.9	62 ± 4	5.8 ± 0.3	94 ± 2
94.0	79 ± 6	6.3 ± 0.2	79 ± 6
100.0	306 ± 14	25.8 ± 0.8	84 ± 3

Figure 2. Distribution of rod aspect ratio, $r = l/d$, vs dispersion temperature T. Dimensions were calculated from measurements of 50 rods, and the error bars correspond to the standard deviation of the measurements. Rod length was extracted from confocal micrographs, and rod diameter was extracted from height profiles of atomic force micrographs (AFM). Rod suspensions with $r = 62$ and $r = 306$ are highlighted on the plot and correspond to the rods shown in Figure 1.

at 100.0 °C is 306 ± 14. Thus, the polydispersity of the rod aspect ratio is approximately 5%. The full dimensions of the rods shown in Figure 1 are reported in Table 1 for all rod suspensions studied.

The AFM micrographs show that the surfaces of rods have texture and the rods appear to have a helical-like structure (Figure 1g,h), similar to other fibrillar systems.[50] Figure 1g shows the surface texture of the rods, and Figure 1h shows the height profile for the cross-section of the rod. The height profile suggests that the rod is a helical ribbonlike structure with a helix pitch length of 100 nm. There is evidence of aggregation in the dried samples regardless of the dilution factor; however, wet images of suspensions of rods observed with confocal microscopy confirm that the rods are not aggregated and are well-dispersed at the single particle level.

Figure 2 presents the variation of the aspect ratio l/d, where l is the length from CLSM and d is the diameter as determined from AFM as a function of preparation temperature. The temperature was varied from 59 to 100 °C. This temperature range gives an order of magnitude variation in the aspect ratio from 11 to 306. Mixing temperatures below 59 °C resulted in poor dispersion of the polyamide powder, and temperatures above 100 °C caused the sample to boil. Rod suspensions with $r = 62$ and $r = 306$ are highlighted on the plot and correspond to the rods shown in Figure 1. The lengths of the rods range from $0.9 < l < 25.8$ μm, and the rod diameter is approximately 80 nm, indicating that the rods grow only in length during preparation. Only rods from $r = 8$ to $r = 79$ were used in this study, since rods of higher r displayed some curvature.

The aspect ratio dependence of the rods on preparation temperature is interesting, and on the basis of our results, we can formulate two possible hypotheses of rod formation. The first

---

(50) Tamura, T.; Suetake, T.; Ohkubo, T.; Ohbu, K. *J. Am. Oil Chem. Soc.* **1994**, *71*, 857–861.

hypothesis is that rods are already present in the polyamide powder; therefore, rod suspensions are formed simply by dispersion of the polyamide powder. To test this hypothesis, we dispersed the powder using sonication and vortex mixing for 15 min at room temperature. Sonication did not result in well-dispersed suspensions, but an increase in turbidity of the surfactant solution confirmed that some of the powder did disperse. Vortex mixing resulted in a very well-dispersed suspension after 1 min of mixing. After the redispersion steps, the samples were observed by CLSM. Although polyamide was present in particle form, no rods were observed (recall Figure 1) as when the surfactant and heating/cooling procedures were applied. The second hypothesis is a thermally and mechanically mediated crystallization of rods in the presence of surfactant. To test this hypothesis, we attempted to produce rods using a quiescent process. After the polyamide powder and surfactant phase were combined, the vial was suspended in a silicon bath at 89 °C for 24 h. The mixture separated into an excess polyamide phase at the top of the vial and a clear aqueous surfactant phase at the bottom of the vial. The clarity of the bottom phase indicated the absence of large aggregates or dispersed phases. The clear phase was removed from the vial, placed on a cover slide, and observed using CLSM. The microstructure of the clear phase was complex with a coexistence of large globules (up to 50 μm) and long strings (up to 50 μm). Thus, we conclude that application of heating alone is not sufficient to produce small, monodisperse rods.

In fact, all of mechanical agitation, heating, and surfactant are required for rod formation. For example, attempts to form rods without adding surfactant or attempts at the synthesis with lower amounts of surfactant (<8% wt) failed to produce rods. Moreover, if the sample was left at a temperature of 89 °C for 24 h after stirring was ceased, the sample phase separated. When the clear phase was removed and observed by CLSM, some rods were present (although not as monodisperse as the rods reported in Figure 1). This result shows that rods form out of the clear phase. This phase may be a microemulsion phase that exists in equilibrium with excess oil present as macroemulsion drops.[51] Furthermore, it is likely that the effect of agitation accelerates diffusion-limited solubilization and controls the degree of particle size uniformity that results from the synthesis. Rods form by microemulsion-templated recrystallization upon cooling.[52]

In light of these tests, the second hypothesis provides the most plausible mechanism for rod formation; however, it does not fully explain the temperature-dependent tunability of the rod aspect ratio. The tunability of r is most likely a consequence of different rod growth rates during cooling. If the system dissolves more material at higher temperatures, the driving force of supersaturation could cause faster rod growth. Even if polyamide solubility does not vary with temperature, cooling from higher temperatures to room temperature allows more time for rod growth than from lower temperatures. As a result, longer rods are produced when starting from higher temperatures. By varying the preparation temperature from $59 < T < 100°$, we obtained rods for which r varied by over a decade ($8 < r < 306$), although at the highest r, the rods were no longer rectilinear. Although it is unlikely that the Disparlon 6650 used here contains the same polyamide used by Demirel and co-workers,[53] it is worth noting that they found highly coagulated fibers using only water as a solvent, whereas
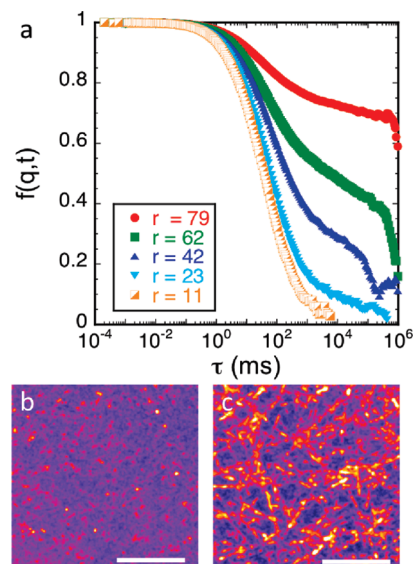

Figure 3. (a) Dynamic structure factor as a function of rod aspect ratio for suspensions of $\phi = 1 \times 10^{-3}$. CLSM micrographs of 10 μm stacks of rod suspensions: (b) $r = 23$ showing no rod network and (c) $r = 79$ showing rod network with connectivity resulting in arrested dynamics. Scale bars are 10 μm.

using surfactant here, we find individual rods. It is likely that the surfactant both aids solubilization of the polymer as well as stabilizes it against coagulation during crystallization.

Effect of Aspect Ratio and Concentration on Suspension Dynamics. The effect of aspect ratio on the dynamic structure factor, $f(q,t)$, is plotted in Figure 3a. The volume fraction of the rod suspensions was $\phi = 0.001$. [From three independent measurements for a rod suspension ($r = 23$), we find that the mean standard error of $f(q,t)$ is 1.73%. Thus, differences in the different samples of Figure 3a are well beyond the measurement error.] Low aspect ratio rod suspensions exhibit fluidlike dynamics since $f(q,t)$ decays to zero. However, for $r \geq 42$, as the aspect ratio is increased, a partial decay to an intermediate plateau in $f(q,t)$ becomes apparent at about 10^3 ms. The existence of a finite plateau in $f(q,t)$ in this interval suggests that the rods are dynamically arrested.[9,54,55] In rod suspensions, possible origins of arrest could be entanglement,[1,2] vitrification,[46] or gelation.[47] Confocal microscopy was used to probe the microscopic structure of the suspensions. Figure 3b shows a Gaussian filtered maximum intensity projection of a 10 μm CLSM image stack of low aspect ratio rods ($r = 23$). The image shows no network connectivity in the suspension. This microstructure is consistent with the fluidlike dynamics observed in $f(q,t)$. The low aspect ratio rods ($r = 11$) also exhibit nearly unconstrained Brownian motion when observed under the microscope.

As r is increased, the prominence and height of the intermediate plateau increase, consistent with constrained dynamics of semidilute suspensions. Figure 3c reports an image stack for high aspect ratio rods ($r = 79$) produced as in Figure 3b. The image stack shows rod network connectivity. Smaller stacks were also produced to ensure that connectivity persisted throughout the sample. Stacks as small as 1 μm showed connectivity between neighboring rods. The CLSM observations also suggest a constrained state, consistent with the observed plateau at intermediate times in $f(q,t)$. Furthermore, at intermediate and high aspect ratios ($r > 23$), there is no resolvable motion of the rods under the

(51) Evilevitch, A.; Olsson, U.; Jonsson, B.; Wennerstrom, H. *Langmuir* **2000**, *16*, 8755–8762.

(52) wook Jun, Y.; Casula, M.; Sim, J.; Kim, S.; Cheon, J.; Alivisatos, A. *J. Am. Chem. Soc.* **2003**, *125*, 15981–15985.

(53) Demirel, A.; Meyer, M.; Schlaad, H. *Angew. Chem., Int. Ed.* **2007**, *46*, 8622–8624.

(54) Krall, A.; Weitz, D. *Phys. Rev. Lett.* **1998**, *80*, 778–781.

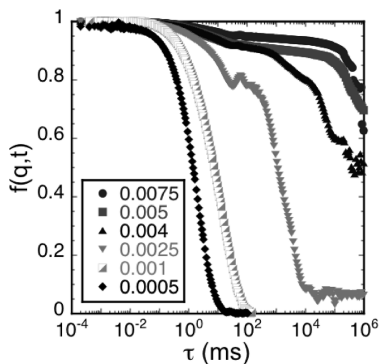(55) Varadan, P.; Solomon, M. *Langmuir* **2001**, *17*, 2918–2929.

Figure 4. Volume fraction dependence of the dynamic structure factor for rods with an of aspect ratio 8. The legend shows the volume fraction of the suspensions. Arrested dynamics occur at $\phi = 0.0025$.

microscope. The dynamic structure factor partially decays for rod suspension with $r = 42$, where $f(q,t) \approx 0.3$ for $\tau \approx 10^2–10^5$ ms. Similarly, for $r = 62$ and $r = 79$, $f(q,t) \approx 0.45$ and $f(q,t) \approx 0.7$ over the same intermediate times. At long times, $f(q,t)$ for suspensions with $r \geq 42$ exhibits a final decay at $\tau > 10^5$ ms. This final decay has been reported in weak colloidal gels of spherical colloids and has been attributed to aging and restructuring within the gels.[56,57] The final decay has also been reported in suspensions of boehmite rods.[9] Figure 3 shows that upon varying the aspect ratio of the rods, the macroscopic structure of the suspensions is tuned from rods with no connectivity and diffusive dynamics to constrained rods with network connectivity and arrested dynamics.

Figure 4 reports the effect of increasing the concentration of low aspect ratio rods ($r = 8$) on the dynamic structure factor. The time scale for the initial relaxation of $f(q,t)$ to its plateau height is a strong function of volume fraction. Also, the figure shows that the height of the plateau in $f(q,t)$ varies with volume fraction. There is an oscillation in $f(q,t)$ for $\phi = 0.0025$ at the intermediate plateau. This is a consequence of low damping of acoustic waves in the sample in this particular dynamical state and is typical in gels.[58] Note that the location of the intermediate plateau corresponds to the amount of arrest in the system. For example, a high plateau indicates that only a small amount of the specimen undergoes displacements of order $2\pi/q$, where $q = 5.94\,\mu m^{-1}$ for this study. Such heavily arrested dynamics observed at a high volume fraction indicates the existence of either entangled, gelled, or glassy states.

Effect of Attractions on Suspension Dynamics. Attractions were induced in rod suspensions with an aspect ratio of $r = 54$ by adding a nonadsorbing polymer. Figure 5 reports the effect of increasing amounts of polymer on the microstructure of the rod suspensions observed using CLSM. The strength of attraction is quantified by the dimensionless polymer concentration c/c^*. As c/c^* is increased, some dramatic structural changes take place. First, Figure 5a−c shows that the addition of attractions promotes networks with increasing connectivity between the rods. At $c/c^* = 0.38$, a striking difference in the structure is apparent. The rod network is replaced by a self-assembled state of large bundled aggregates. Individual rods are also present. The large bundles are made up of several rods. The rods order nematically within the bundle, and the micrographs indicate that the bundles are several rod diameters wide and 1−2 rod lengths long (Figure 5d).
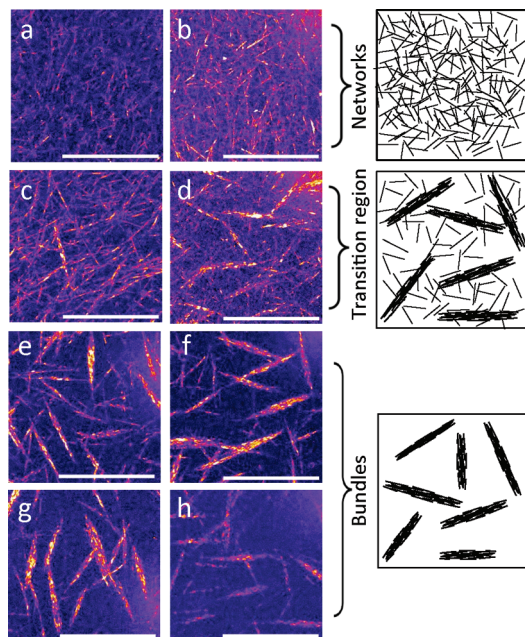
(56) Solomon, M. J.; Varadan, P. *Phys. Rev. E* **2001**, *63*, 051402.
(57) Cipelletti, L.; Manley, S.; Ball, R.; Weitz, D. *Phys. Rev. Lett.* **2000**, *84*, 2275–2278.
(58) Sztucki, M.; Narayanan, T.; Belina, G.; Moussaïd, A.; Hoekstra, H. *Phys. Rev. E* **2006**, *74*, 051504.

Figure 5. CLSM micrographs of rod suspensions ($r = 54$) as a function of U/k_BT with $\phi = 0.001$. (a) No polymer, (b) $c/c^* = 0.014$, (c) $c/c^* = 0.14$, (d) $c/c^* = 0.38$, (e) $c/c^* = 0.52$, (f) $c/c^* = 0.71$, (g) $c/c^* = 0.93$, and (h) $c/c^* = 1.19$. Increasing the c/c^* of the polymer solution induces homogeneous structural transitions in the rod suspensions. Scale bars are 10 μm.
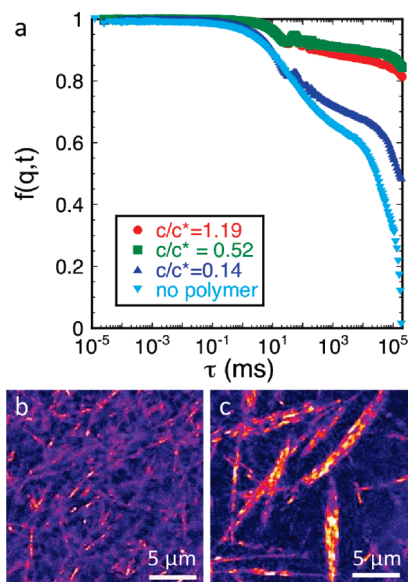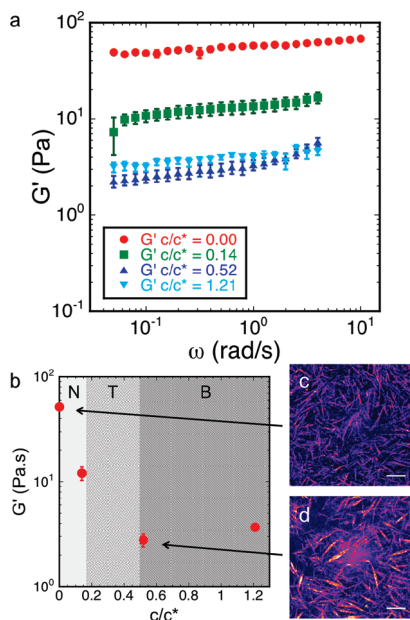

Figure 6. (a) Dynamic structure factor as a function of increasing polymer concentration, i.e., increasing U/k_BT for suspensions with $r = 54$. (b) CLSM micrograph showing a close-up of the rod network with no added polymer. (c) CLSM micrograph showing a close-up of the bundled structures for a rod suspension with $c/c^* = 0.52$. The scale bar is 5 μm.

Increasing c/c^* beyond the critical value of $c/c^* = 0.38$ results in a homogeneous phase of large bundles of rods. Once bundles are formed, further increases in c/c^* do not induce any discernible differences in the bundled structures.

Figure 6 reports the effect of added attractions on the rod dynamics at $q = 13.1\,\mu m^{-1}$ and for $r = 54$. (Recall that at this q, DLS probes fluctuations of order of a half micrometer, about one-tenth the scale of the rod length.) For no added polymer, at this volume fraction ($\phi = 0.001$), $f(q,t)$ is consistent with an

Figure 7. (a) Storage modulus for a rod suspension ($r = 39$) of varying c/c^* at $\phi = 0.015$. Standard errors of the mean are reported from three independent experiments. (b) Reports average storage moduli between $0.1 < \omega < 0.5$ vs c/c^* for the suspensions. The plot is separated into regions of different structure. *N* corresponds to rod networks, *T* correponds to the transition region where networks and bundles coexist, and *B* corresponds to rod bundles. Single slice CLSM micrographs of (c) $c/c^* = 0.00$ and (d) $c/c^* = 0.52$. The scale bar is 10 μm. The suspensions correspond to the samples used in Figure 7a and thus have a concentration 15 times higher than suspensions previously observed using CLSM.

intermediate regime [$f(q,t) \sim 0.6$ for $\tau \approx 10^2 - 10^4$ ms] of slow dynamics followed by a decay to the baseline, consistent with fluid behavior. The addition of polymer at a concentration of $c/c^* = 0.14$ (an amount that leads to the structure shown in the image of Figure 5c) induces only modest changes in $f(q,t)$. The intermediate region is higher, and the decay to fluid behavior takes slightly longer. However, increasing the rod attractions further by adding polymer at $c/c^* = 0.52$ produces larger changes in $f(q,t)$. In this case, $f(q,t)$ only decays by about 15% over the full 10^5 ms of the experiment. As c/c^* increases further, little change in the dynamic structure factor occurs, as evidenced by the fact that $f(q,t)$ for $c/c^* = 0.52$ and $c/c^* = 1.19$ nearly overlay. The significant changes in dynamic structure reported in Figure 6a occur over attraction strengths that also induce structural changes in the rod suspensions. Figure 6b,c shows details of reflection CLSM of structure at this volume fraction for $c/c^* = 0$ and $c/c^* = 0.52$. Comparing Figure 6a−c, it is apparent that the increasingly incomplete relaxation in the dynamic structure (Figure 6a) caused by increasing the depletion attraction is linked to the formation of the bundles apparent in the CLSM images.

Rheology. Figure 7a compares the storage modulus (G') of rod suspensions ($r = 39$) with no added attractions (no polymer) and with added attractions ($c/c^* = 0.14$, 0.52, and 1.21) at $\phi = 0.015$. The nearly frequency-independent results suggest that the measurements have been performed at frequencies greater than the crossover. (In fact, the storage modulus is greater than the loss modulus, $G' > G''$, in this frequency regime.) Throughout this frequency regime, added attractions cause an order of magnitude decrease in the storage modulus of the suspension. Figure 7b shows average G' for rod suspensions with increasing c/c^*. The plot can be separated into regimes of different microstructure as deduced from Figure 5. At $c/c^* \leq 0.14$, the microstructure of the

suspension corresponds to a rod network (N). For $0.14 \leq c/c^* \leq 0.52$, the suspension corresponds to a coexistence of rod network and rod bundles (T). Finally, $c/c^* \geq 0.52$ corresponds to rod bundles (B). Suspensions in the first regime, N, typically exhibit $G' \approx 60$ Pa, whereas suspensions in B typically exhibit $G' \approx 4$ Pa.

Figure 7c,d are CLSM micrographs of the suspension with $c/c^* = 0.00$ and the suspension with $c/c^* = 0.52$, respectively. The micrographs highlight differences in the microstructures of the suspensions. Figure 7c ($c/c^* = 0.00$) identifies a homogeneous rod network typical for polyamide rod suspensions of $r > 23$. Figure 7d ($c/c^* = 0.52$) identifies rod bundles with structureless voids around the bundles. The change in the structure of the suspensions corresponds to an order of magnitude drop in G'. The structureless voids could contribute to a drop in G' because adding attractions induces bundle formation.

Discussion

This polyamide system opens new possibilities to explore the effect of aspect ratio, r, volume fraction, ϕ, and interaction potential, c/c^*, on properties such as microscopic structure and dynamics of rod suspensions. We found that relatively small increases in r, ϕ, and c/c^* resulted in the slowing down of the dynamics of the rods as well as changes in the structure of the rod suspensions. The behavior of the dynamic structure factor for rod suspensions at low r and ϕ was consistent with fluidlike dynamics in which the particles diffused freely. As r and ϕ are increased, $f(q,t)$ deviated from a fluidlike profile in a way that was consistent with dynamical arrest in the suspension. Increasing c/c^* also induced arrested dynamics. Mohraz and Solomon reported similar results for boehmite spindles of $r = 3.9$, 8.6, and 30.1.[9] That study reported that the dynamics of rod aggregates are far more complex than the dynamics of spherical aggregates[54,56,57] due to the anisotropic excluded volume of rods. They showed that increasing r decreased the minimum volume fraction required for gelation. The microstructure was not observed in this study, but the dynamic structure factor was consistent with that of a constrained fractal structure. Furthermore, simulations of low aspect ratio rod suspensions ($r = 8$) resulted in fractal clusters.[14]

Our observations from CLSM confirmed that the structure varied from a fluidlike suspension of rods, which exhibited Brownian dynamics and did not appear to interact with each other, to a rod network wherein the rods had network connectivity. The CLSM micrographs showed that increasing r and ϕ induced a highly constrained rod network. We did not observe any evidence for fractal structure or long-range heterogeneity in this system at the r, ϕ, and c/c^* studied. Thus, slow and arrested dynamics in gels can have multiple origins.

Modest changes in the interaction potential between rods significantly altered the physical state of the rod suspensions.[59] Adding attractions may result in several different structures in rod suspensions: The first possible structure is that of a homogeneous network of rods. Homogeneous networks have been inferred by small angle neutron scattering in dilute suspensions of surfactant-stabilized single wall carbon nanotubes (SWNTs).[60] The second possible structure consists of hetrogeneous networks of fractal aggregates or clusters. Fractal aggregates have been inferred from power law dependence of the structure factor [$S(q)$] in boehmite rods.[9] The third possible structure corresponds to bundles of rods, as observed here. In bundles, rods take a side by side conformation as though there is local nematic ordering.[32] Bundles have

(59) Russel, W. B.; Saville, D. A.; Schowalter, W. R. *Colloidal Dispersions*, 1st ed.; Cambridge University Press: Cambridge, 1991.
(60) Zhou, W. *Chem. Phys. Lett.* **2004**, *384*, 185–189.

been observed in CNTs,[61] *f*-actin,[62] and most recently in *fd* virus.[32] Because transitions among these three structures are rarely observed in the same system, little is known about the conditions required to produce one or the other. The aspect ratio and strength of interaction dependence on structural transitions are also poorly understood. For example, the differences in system conditions that lead to fractals and the conditions that lead to bundles are not known. It appears that r and c/c^* would be good candidate parameters for possible ways to control the structure of rod suspensions.

By adding a nonadsorbing polymer to the polyamide rod suspensions, a depletion interaction between the rods was induced. The depletant was added to the rod suspension and slowly rolled for 24 h (less than 3 rpm). The bundles formed during the mixing process; however, bundles also formed when the suspensions were rolled for less time, as little as 1 h. If the depletant and rod suspension were not mixed thoroughly, bundles did not form. Therefore, there is some suggestion from the measurements that the bundling transition has a kinetic component.

The macroscopic structure of the rod suspensions varied from a homogeneous rod network to a phase of "granular"-sized bundles that were noncolloidal. Although both structures have voids/pores on the scale of the rod, they appeared homogeneous on a large scale. This situation is unlike heterogeneous fractal clusters observed in other rod systems, which are heterogeneous on large length scales.

We found that the bundles were aggregates of individually oriented rods. Further dilution of the bundled system with DI water caused the aggregates to break up. This break up indicated that the structural transition was reversible. Depletion-induced bundling of rods has been observed in other systems including *f*-actin.[62] Bundles in *f*-actin were induced either using a bundling agent [for example, a polycation of basic polypetide,[63] by *f*-actin binding proteins (ABPs)[64]] or by using a polymer depletant.[62] In the first two examples, the electrostatic interaction between actin filaments was varied, and a transition from a single filament state to a bundled filament state was observed. However, in the final example, a polymer depletant was used to tune the interaction between rods. A progressively bundled state was formed and observed using phase contrast microscopy; however, the transition between *f*-actin networks and *f*-actin bundles was not observed in detail due to particle size constraints.[62]

The bundles formed in the polyamide system differ significantly from bundles formed in *f*-actin. First, they self-organize into ordered bundles of rods, which themselves have a rodlike appearance. By contrast, *f*-actin appears to maintain a rod network structure even when bundled.[62] Second, as the interaction potential strength is increased, a region of coexistence between individual rods and rod bundles is observed for polyamide rods. Such varying degrees of bundling do not appear to exist in *f*-actin networks. Third, the bundles have a finite size, and further increases in c/c^* do not affect the dimensions of the bundles. They are several rod diameters wide and 1−2 rod diameters long. Finally, the bundles did not exist in a network at the rod concentrations studied here. Instead, they aggregated into single bundles with limited physical connectivity between adjacent bundles. (However, note that measurement of the linear viscoelasticity of the suspensions indicates that the bundles must still interact with the neighboring bundles since the suspension of rod bundles exhibited a measurable elastic modulus.)

Thus, we have shown that modest changes in interaction potential in rods induced bundles and the effect on the macroscopic structure of the suspensions is dramatic. Bundle formation has serious implications for complex fluid formulation. Rods are typically added to formulations as structurants to prevent sedimentation of the products. Inadvertent bundle formation could result in undesirable material properties. They are also an inefficient use of material since a larger volume fraction of rods is required for gelation due to the higher density of the bundles.

What consequences does adding attractions have for the linear viscoelasticity of the polyamide rod suspensions? Pair potentials have previously been varied in rod suspensions as a means to increase their linear elastic modulus. For example, Fan and Advani[24] found that the addition of salt to stable suspensions of CNTs increased the moduli by an order of magnitude. Using both TEM and a capillary-based method,[65] they concluded that the increased modulus was due to increased connectivity in the CNT network. Adding attractions in other colloidal suspensions has also been shown to induce aggregation and increase the moduli of suspensions.[9,24,66]

Conversely, in the polyamide rod suspensions studied here, adding attractions via the depletion interaction decreased the storage modulus of the suspensions as in Figure 7. This result is counterintuitive relative to the previous discussion and the literature. However, from inspection of the CLSM micrographs, a hypothesis that explains the drop in the storage modulus emerges. These micrographs show that although the added attractions do indeed induce aggregation, voids of rods are also induced due to the bundling transition. The voids exist because the number of rods in the suspension is fixed. Adding attractions induces the formation of bundles, which are nematically ordered aggregates of rods and thus have a higher density. The bundles are surrounded by structural voids, which contribute to a drop in the elastic modulus of the suspension. Furthermore, the effect of densifying rods into bundles leads to an apparent drop in the number of contacts per rod where the number of contacts is related to the moduli of the suspension.[67] Therefore the network structure that is present in the suspension with no added attractions (no polymer, Figure 5c) has a larger storage modulus because the rod network is homogeneous. This result, in which elasticity is decreased by added attractions, is qualitatively similar to the re-entrant behavior of colloidal suspensions at the glass transition when attractions are added. Pham and co-workers suggest that added attractions modify the cage structure of concentrated colloids, thereby resulting in melting of the glass.[68] Here, a similar loss of elasticity occurs through a structural transition from networks to bundles induced by the depletion attraction.

To conclude, we note that further study is required to discover what drives different aggregate structures in rod suspensions. For example, it would be of interest to map out a phase diagram of regions in which each structure is achieved. Apparently, fractals, clusters, networks, and bundles are all possible conformations of rod aggregates. More work is required to understand the different pathways by which these structures form and understand the dynamics of these arrested structures. Finally, we suggest that the system used here, and the measurements performed, could equally

(61) Luo, Z.; Li, R.; Kim, S.; Papadimitrakopoulos, F. *Phys. Rev. B* **2004**, *70*, 245429.
(62) Hosek, M.; Tang, J. *Phys. Rev. E* **2004**, *69*, 051907.
(63) Tang, J. X.; Janmey, P. A. *J. Biol. Chem.* **1996**, *271*, 8556–8563.
(64) Shin, J.; Gardel, M.; Mahadevan, L.; Matsudaira, P.; Weitz, D. *Proc. Natl. Acad. Sci.* **2004**, *101*, 9636.

(65) Fan, Z.; Hsiao, K.; Advani, S. *Carbon* **2004**, *42*, 871–876.
(66) Djalili-Moghaddam, M.; Toll, S. *Rheol. Acta* **2006**, *45*, 315–320.
(67) DiDonna, B.; Morse, D. arXiv:cond-mat/0703418v1, 2007.
(68) Pham, K.; Egelhaaf, S.; Pusey, P.; Poon, W. *Phys. Rev. E* **2004**, *69*, 011503.

well be applied to the study of glassy rod systems by concentrating the rod suspensions through a technique such as centrifugation.